A SURROGATE MODEL FOR HEAT-EXCHANGER USING NON-INTRUSIVE REDUCED ORDER MODELLING

Shri Balaji Padmanabhan[1]*, Mohamed Tahar Mabrouk[1], Bruno Lacarrière[1]

[1]IMT Atlantique, Department of Energy Systems and Environment, GEPEA, UMR CNRS, 6144, F-44307 Nantes, France

*Corresponding Author: shri-balaji.padmanabhan@imt-atlantique.fr

ABSTRACT

Dynamic modeling of heat exchangers is crucial in developing accurate models of various energy systems such as chillers, heat pumps and its other standalone applications. The operational efficiency and accuracy of the dynamic heat exchanger model relies heavily on the numerical method used in solving it. Among the common numerical approaches used in dynamic modeling of the heat exchanger, finite volume (FV) method is found to be more robust and highly accurate, but it falls short in terms of computational efficiency when compared to others. Fast and accurate dynamic model of heat exchanger is essential for effective model-based control, system optimization and real time monitoring. This paper presents a surrogate model for a refrigerant-water heat exchanger using non-intrusive reduced order modeling with Radial Basis Function (RBF) regression and a Deep Neural Network (DNN). The surrogate model is specifically designed to handle step-like variations in input. Moreover, it provides solution with good accuracy, with a mean absolute error of around 0.35 K on the secondary fluid outlet temperature solution, while providing dramatically faster computation speed that are 150 times faster than FV approach for dynamic heat exchanger model. The proposed modeling approach is general and easily applicable to modeling of the heat exchangers for different configurations, and compatible for receding horizon model control.

1 INTRODUCTION

Heat exchangers facilitate effective heat transfer between two or more fluids, or between a fluid and a solid, when they are at varying temperatures. They have a broad spectrum of applications across various sectors such as HVAC (Heating, Ventilation, and Air Conditioning), chemical processing, automotive systems, renewable energy systems like solar and geothermal power plants. It is an important component of various vapor compression systems (chillers and heat pump). The dynamics behavior of these systems is largely contingent upon the heat-exchangers (evaporator / condenser). Accurate and efficient modeling of the heat-exchanger is crucial in developing dynamic models of vapor compression systems. It is highly challenging to model the dynamics of heat-exchangers, particularly when the primary fluid is compressible and also phase change occurs. Consequently, the accuracy and computational efficiency of vapor compression system models depend significantly on the approach taken to solve the dynamic heat exchanger model.

The common approaches used in dynamic modeling of heat-exchanger are Lumped Parameter (LP) method (Braun, 1988) (Jin & Spitler, 2002), Moving Boundary (MB) method (Grald & MacArthur, 1992) (He et al, 1994) (Pettit et al ,1998) and Finite Volume (FV) method (MacArthur & Grald, 1987) (Rossi & Braun, 1999). The Lumped Parameter method simplifies the heat exchanger into a system with aggregated thermal properties and assuming uniform temperature distribution in each lump. The LP model is easy to solve and straightforward but it highly lacks accuracy. Specifically, it does not account for phase changes in two-phase fluids. In the MB method, the heat-exchanger is divided into three zones/regions namely vapor, two-phase and liquid. Each region has its respective conservation equations to solve. The boundaries of these regions are dynamically adjusted while solving. This method is quite fast and has reasonable accuracy. The LP and MB methods are primarily developed for real time application like model control. In these methods, the model complexity is decreased for faster

https://doi.org/10.52202/077185-0088

simulation but which is also results in loss of accuracy. In the FV method, the heat exchanger is discretized into n number of control volumes and solved, allowing for the precise calculation of heat transfer and fluid flow at each volume. It is highly versatile and identified as the most accurate, yet it is also computationally expensive option (Bendapudi et al, 2008). For the purpose of model control of vapor compression systems, there is a need for faster dynamic model of heat exchanger that has the accuracy of FV model.

Reduced order modeling (Chinesta et al, 2010) (Bergmann et al, 2005) is one of the possible ways to accelerate models without sacrificing their accuracy. ROM aims at lowering the dimension of a computational problem while preserving its input-output behavior as much as possible. The ROM will have a much smaller dimension than a high-fidelity approximation space. Thus, it computes the solution much faster with limited computational power than solving the high-fidelity full order problem and has a reliable outcome. The accuracy and efficiency of the ROMs mostly depend on the choice of the type of ROM. There exist many kinds of ROMs, such as Proper Orthogonal Decomposition - POD (Chatterjee, 2000), Dynamic mode decomposition (Schmid, 2010), Proper Generalized Decomposition (Chinesta et al, 2010). Among these, the most popular option is POD, which is a posteriori model reduction technique. POD is aimed at reducing a large number of variables to a much smaller number of uncorrelated variables, while retaining as much as possible variation in the original variables. In POD, there are two main model construction techniques Intrusive POD (Volkwein, 2013) and Non-Intrusive POD (Audouze, 2013). In Intrusive POD, a new low dimensional system of equations is built by projecting the original system of equations into a low dimensional reduced space. Solving this low-dimensional system will be less expensive than the original full-order system. Whereas, Non-Intrusive POD method is independent of the governing equations. Here, instead of projecting the system of equations into low-dimensional space, the solution is approximated with the help of machine learning methods.

There have been quite few studies in the literature about building ROM based on Intrusive POD for heat exchanger model. Alonso et al (2009) have developed robust reduced order modeling for steady state heat transfer problems using POD and genetic algorithms. Xu et al (2018) have implemented ROM for the heat exchanger model using Intrusive POD technique. Samadiani and Joshi (2010) also used Intrusive POD based ROM to model steady state heat transfer in data centers for turbulent flows. In addition to POD based ROM, several other techniques have also been explored to develop ROMs for heat exchanger models. Baldea and Daoutidis (2006) have built a reduced model for reactor-heat exchanger networks by employing singular perturbation theory to analyze the system's dynamics. Majumdar et al. (2018) explored the dynamics of two-phase flows within a narrow tube heat exchanger using a quasi-steady state reduced order model. To the best of the authors' knowledge, there has been no existing literature that specifically addresses the reduced order modeling of heat exchanger using Non-Intrusive method. In this study, a surrogate model of dynamic heat exchanger is developed using Non-Intrusive ROM technique with Radial Basis Function (RBF) regression and a Deep Neural Network (DNN). Here the DNN corrects the errors made by the ROM on quantity of interest, making this modeling approach as a sequential ensemble machine learning technique.

2 HEAT-EXCHANGER MODELING

The dynamic modeling of heat exchanger includes mass and energy conservation laws applied to the primary fluid, and energy conservation for the secondary fluid and the primary fluid’s tube. The heat exchanger is modelled for a compressible primary fluid and incompressible secondary fluid. And the pipes are made of copper. The flow directions of the fluids are considered as parallel.

The following assumptions are made to model the dynamics of a heat-exchanger,

1. The heat exchanger is assumed to be a long, thin and horizontal tube such that the refrigerant flows inside can be modeled as a one-dimensional fluid flow.

https://doi.org/10.52202/077185-0088

2. The pressure drops along the length of the heat exchanger due to change in momentum of refrigerant or due to viscous friction is assumed to be negligible.
3. The axial conduction of heat is less when compared to the heat transfer between fluids and tube, so it is not modeled.

Based on these assumptions, the conservation equations for primary fluid, secondary fluid and tube are given as following,

$$\frac{\partial \rho_p}{\partial t} + \frac{\partial (\rho v)_p}{\partial z} = 0 \tag{1}$$

$$\frac{\partial (\rho h - P)_p}{\partial t} + \frac{\partial (\rho h v)_p}{\partial z} + \frac{\partial \left(\alpha_{pw}(T_p - T_w)\right)}{\partial z} = 0 \tag{2}$$

$$\left(C_p \rho A\right)_w \frac{\partial T_w}{\partial t} - \frac{\partial \left(\alpha_{pw}(T_p - T_w)\right)}{\partial z} + \frac{\partial \left(\alpha_{ws}(T_w - T_s)\right)}{\partial z} = 0 \tag{3}$$

$$\left(C_p \rho A\right)_s \frac{\partial T_s}{\partial t} + \left(C_p \rho A v\right)_s \frac{\partial T_s}{\partial z} - \frac{\partial \left(\alpha_{ws}(T_w - T_s)\right)}{\partial z} = 0 \tag{4}$$

2.1 Finite Volume Formulation

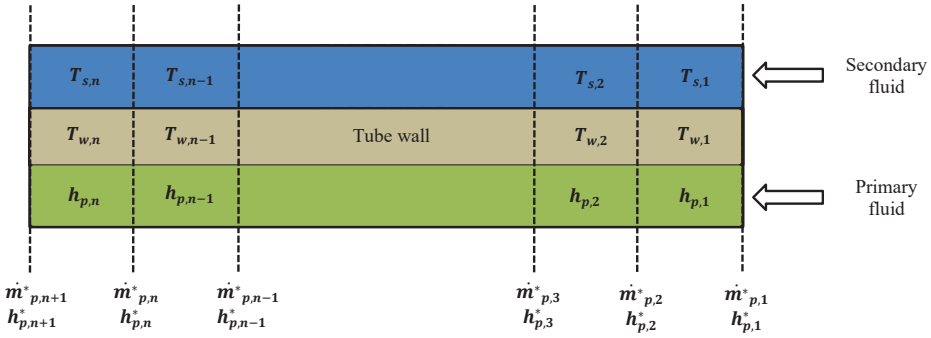

Figure 1: Discretized heat exchanger model

In FV, the heat-exchanger is divided into a number of control volumes along the length. In the discretization process, two types of variables are used: cell variables and node variables. The node variables are indicated by a "$*$" superscript. In this study, a linear profile for both enthalpy and mass flow rate across all elementary control volumes is considered. Thus, the values of enthalpy and mass flow rate at the cell center are determined as follows,

$$h_{p,k} = \frac{h^*_{p,k} + h^*_{p,k+1}}{2}; \qquad \dot{m}_{p,k} = \frac{\dot{m}^*_{p,k} + \dot{m}^*_{p,k+1}}{2}$$

Figure 1 illustrates the discretized one-dimensional shell and tube heat-exchanger. By integrating the conservation equations $(1) - (4)$ over the control volumes and after applying the simplifications, the following coupled linear set of Ordinary Differential Equations (ODEs) for k^{th} control volume is obtained (Bendapudi et al, 2008).

$$a_k \frac{dP_p}{dt} + b_k \frac{dh_{p,k}}{dt} = \dot{m}^*_{p,k-1} - \dot{m}^*_{p,k} \tag{5}$$

https://doi.org/10.52202/077185-0088

$$c_k \frac{dP_p}{dt} + d_k \frac{dh_{p,k}}{dt} = \dot{m}^*_{p,k-1} h^*_{p,k-1} - \dot{m}^*_{p,k} h^*_{p,k} - A_{pw,k} \alpha_{pw,k}(T_{p,k} - T_{w,k}) \quad (6)$$

$$(Cp\ \rho\ A)_w \frac{dT_{w,k}}{dt} = A_{pw,k} \alpha_{pw,k}(T_{p,k} - T_{w,k}) - A_{ws,k} \alpha_{ws,k}(T_{w,k} - T_{s,k}) \quad (7)$$

$$(Cp\ \rho\ A)_s \frac{dT_{s,k}}{dt} = \dot{m}_{s,in} Cp_s(T_{s,k-1} - T_{s,k}) + A_{ws,k} \alpha_{ws}(T_{w,k} - T_{s,k}) \quad (8)$$

Where the coefficients are defined as,

$$a_k = V_{p,k} \left(\frac{\partial \rho_{p,k}}{\partial P_{p,k}}\right)_{h_{p,k}} ; \quad b_k = V_{p,k} \left(\frac{\partial \rho_{p,k}}{\partial h_{p,k}}\right)_{P_{p,k}} ; \quad c_k = V_{p,k} \left(h_{p,k} \left(\frac{\partial \rho_{p,k}}{\partial P_{p,k}}\right)_{h_{p,k}} - 1 \right)$$

$$d_k = V_{p,k} \left(\left(\frac{\partial \rho_{p,k}}{\partial P_{p,k}}\right)_{P_{p,k}} + \rho_{p,k} \right)$$

In total, for n control volumes, there are (4 x n) equations and (4 x n) unknowns. The system of equations in matrix form,

$$\vec{A} * \vec{X} = \vec{B} \text{ with } \vec{X} = \left[P, h^*_{p,1}, \dots, h^*_{p,n}, \dot{m}^*_{p,2}, \dots \dot{m}^*_{p,n-1}, T_{w,1}, \dots, T_{w,n}, T_{s,1}, \dots, T_{s,n}\right]^T.$$

3 SURROGATE MODEL FOR HEAT-EXCHANGER

The surrogate model is specifically designed to handle sequence of inputs parameters which undergoes step-like variations. Figure 2 shows the input sequence which varies in a step like fashion, where each step is called as an input step with $\boldsymbol{t_{is}}$ being time length of an input step. Figure 3 illustrates the schematic workflow for processing a sequence of input over a time period. Initially, the first input step's initial conditions (IC) for all state variables $\left(\boldsymbol{P^{1\times1}_{p,init}}, \boldsymbol{h^{1\times n}_{p,init}}, \boldsymbol{T^{1\times n}_{w,init}}, \boldsymbol{T^{1\times n}_{s,init}}\right)$ are together condensed into a reduced form (IC_{red}) using Principal Component Analysis – PCA (Zou et al, 2006). The IC_{red}, along with the primary inputs, is fed into the surrogate model, which then produces the solution for the entire time length corresponding to the respective input step. The final solution for the first input step serves as the IC for the second input step, then solution is approximated for second input step. This process is iteratively applied to each following steps in the sequence.

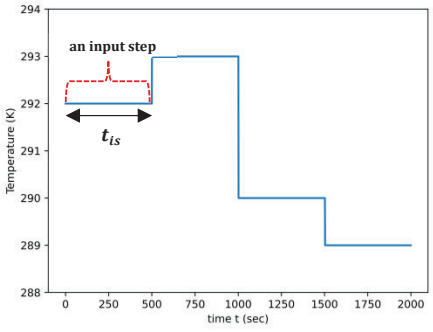

Figure 2: Example of an input sequence of a parameter (inlet temperature) that consists of 4 input steps

https://doi.org/10.52202/077185-0088

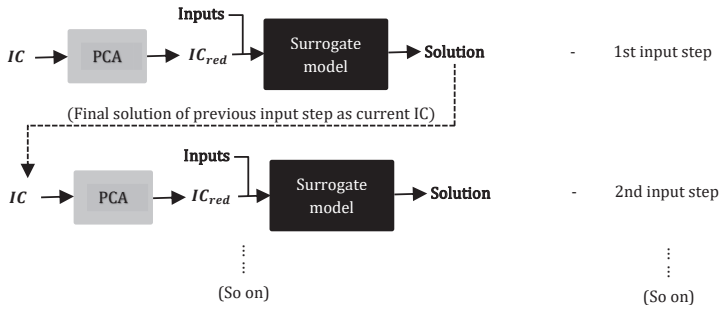

Figure 3: Schematic workflow for a sequence

Figure 4 gives the detailed diagram of the surrogate model (ROM + DNN). Surrogate model includes two blocks, the first is a ROM based on Non-Intrusive POD method which uses RBF regression and later is an error correction unit which contains a DNN. The principal function of the error correction unit is to correct the errors made by the ROM, particularly in the quantity of interest with respect to the inputs. In heat exchanger modeling, the quantity of interest is secondary fluid's outlet temperature ($T_{s,out}$). The quantity of interest can also be the values of any other variables. Thus, along with the primary inputs, DNN takes $T_{s,out}$ from the ROM's output and produces the corrected quantity of interest $T_{s,out}^{new}$.

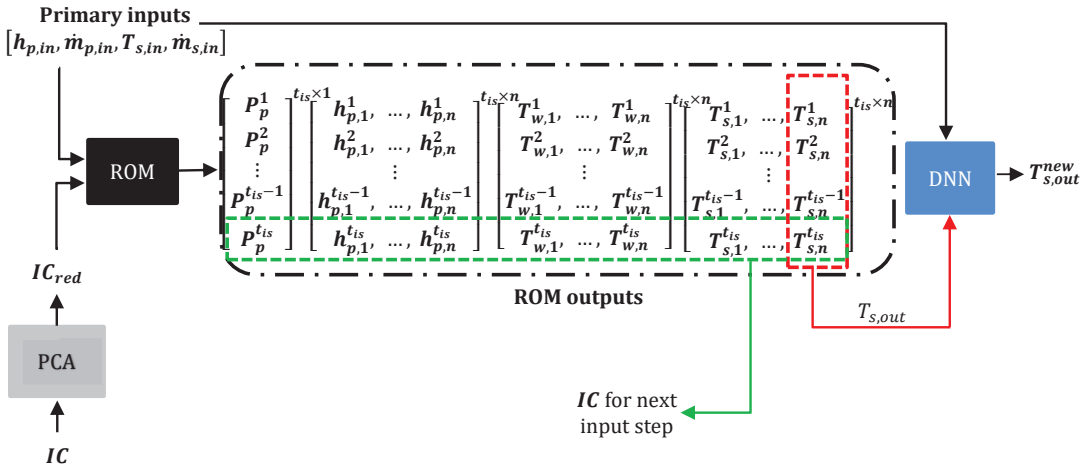

Figure 4: Detailed diagram of the surrogate model

3.1 Reduced Order Model

The ROM built in this study is based on non-intrusive technique which uses POD to decompose the data and then a machine learning method is used to predict the low dimensional features. The brief methodology and mathematical formulation used in building ROM are discussed below.

3.1.1 Mathematical formulation of POD: The mathematical formulation of the POD presented here closely follows Chatterjee (2000) and Audouze (2013). In POD, the solution u for a given parameter ξ is approximated as linear superposition with a set of optimal orthogonal basis vectors ϕ (also called a POD basis functions or POD modes) and the corresponding projection coefficients g. The mathematical formulation of the POD is given as following,

$$u(\xi) \approx \hat{u}(\xi) = \sum_{l=1}^{L} g_l(\xi)\phi_l \tag{9}$$

https://doi.org/10.52202/077185-0088

where L is the optimal number of the POD modes used, the number of POD modes to keep L can be determined based on the decay of first L eigenvalues with respect to the largest eigenvalue, which should be lesser than a pre-defined tolerance level ϵ. If the chosen sequence of basis functions ϕ are orthogonal to each other, then the projections coefficients g_l are found by computing the scalar product between the corresponding solution u and the basis functions ϕ_l. Here $< , >$ denotes scalar dot product.

$$g_l(\xi) = < u(\xi), \phi_l > \tag{10}$$

and the approximated solution $\hat{u}$ can be written as,

$$\hat{u}\,(\xi) = \sum_{l=1}^{L} < u(\xi), \phi_l > \phi_l \tag{11}$$

The POD modes are found by decomposing the specifically arranged solution matrix S (snapshot) using Singular Value Decomposition – SVD (Johnson, 1963). In non-intrusive POD, the projection coefficients $g_l(\xi)$ are predicted by using machine learning methods. In the POD representation, it is supposed that u is known for different $\xi = \{\xi_1, \xi_2, \dots, \xi_m\}$. The objective is to predict the value of u_{new} for the new parameter ξ_{new} which corresponds to a new set of primary inputs.

$$u_{new}\,(\xi_{new}) = \sum_{l=1}^{L} g_l(\xi_{new})\phi_l \tag{12}$$

Machine learning methods such as neural networks, regression methods like Gaussian Process Regression, Radial Basis Function regression can be used to predict the coefficients.

3.1.2 Radial Basis Function (RBF) Regression: For this study, RBF regression has shown superior performance compared to machine learning models and has therefore been selected. Radial Basis Functions (RBF) regression was first introduced by Hardy (1971). RBF regression approximates a function by fitting a linear weighted combination of radial basis functions. The prediction of projection coefficients given new input parameter ξ_{new} is as following,

$$g_l(\xi_{new}) = \sum_{i=1}^{M} w_i\ \Phi\,(||\xi_i - \xi_{new}||) \tag{14}$$

Where ξ_i are set of all training inputs, Φ is a priori chosen basis function, w_i are regression weights and $\|.\|$ refers to Euclidean distance. Commonly used basis functions include multiquadric, Inverse quadrics, Inverse multiquadric, Gaussian, cubic. In this study gaussian is used as regression basis function, which is $\Phi(r) = e^{-(\epsilon r)^2}$. In the training stage, for each training input ξ_j, the regression is written in the form as,

$$g_l(\xi_j) = \sum_{i=1}^{M} w_i\ \Phi\left(||\xi_i - \xi_j||\right) \tag{14}$$

The above equation is given in matrix form as follows G = WB, where B matrix is basis function of Euclidean distance between each and every training inputs. The regression weights W is found by fitting the regression model using least-square method $E(W) = \|G - BW\|^2$. After optimizing the regularized least square function, the optimal regression weights W which minimizes $E(W)$ with λ being the regularization parameter to avoid overfitting is given as $W = [(B^T B + \lambda I)^{-1} B^T G]$. The parameters of the RBF regression model, such as ϵ and λ are tunable hyperparameters.

3.1.3 Training data generation for ROM: The primary inputs for the dynamic heat-exchanger model are refrigerant's inlet enthalpy $h_{p,in}$ and inlet mass flow rate $\dot{m}_{p,in}$, water's inlet temperature $T_{s,in}$ and inlet mass flow rate $\dot{m}_{s,in}$. To generate training data, numerous sequences of simulations are conducted by varying all the primary inputs together. Each sequence begins with randomly chosen initial conditions for the state variables. Here, the key strategy is to keep the time length of each input step to be a fixed constant which is denoted as $t_{is,const}$. The heat exchanger is configured to heat the

https://doi.org/10.52202/077185-0088

secondary fluid (water) by transferring heat from the primary fluid (R410A) through pipe wall made of copper. Physical properties of R410A are calculated with help of CoolProp (Bell et al.). The ranges for selecting the primary inputs are specified in Table 1.

Table 1: Range for varying primary inputs

Primary inputs/ State variables	Range
$\dot{m}_{p,in}$	$1.0\ to\ 1.5\ [kg\ s^{-1}]$
$h_{p,in}$	$3.75e^{+05}\ to\ 4.25e^{+05}\ [J\ kg^{-1}K^{-1}]$
$\dot{m}_{s,in}$	$0.25\ to\ 0.55\ [kg\ s^{-1}]$
$T_{s,in}$	$283\ to\ 300\ [K]$

3.1.4 Building and training of ROM: The training set D_1, consists of data collected from 20 sequences of simulations, each containing 20 continuous input steps. The time length of every input step is fixed to a constant time, denoted as $t_{is,const}$. Here, $t_{is,const}$ is the time taken by the system to reach steady state given an input. The synthetic data is arranged in a specific way to create the snapshot matrix (S) for the ROM. The dynamic solution of state variables for all control volumes for every stepwise variation in inputs within each sequence are flattened and organized in columns. Since the time length of each input step variation is constant, the length of all the columns of S will be the same. For the inputs $\xi_{j=1\ to\ M}$ with each ξ being set of inputs corresponding to M number of input step pairs, S is given as,

$$S = \begin{bmatrix} \begin{bmatrix} P_p \\ h_p \\ T_w \\ T_s \end{bmatrix}^{\xi_1} & \begin{bmatrix} P_p \\ h_p \\ T_w \\ T_s \end{bmatrix}^{\xi_2} & \cdots & \cdots & \begin{bmatrix} P_p \\ h_p \\ T_w \\ T_s \end{bmatrix}^{\xi_{M-1}} & \begin{bmatrix} P_p \\ h_p \\ T_w \\ T_s \end{bmatrix}^{\xi_M} \end{bmatrix}$$

The POD modes (ϕ) can be computed by performing SVD to snapshot matrix S. The decomposition is given by $S = U \Sigma V^T$, where, $S \in \mathbb{R}^{N \times M}$ is the snapshot matrix, $U \in \mathbb{R}^{N \times N}$ is the left orthogonal matrix, $\Sigma \in \mathbb{R}^{N \times M}$ is diagonal matrix of singular values, $V \in \mathbb{R}^{M \times M}$ is the right orthogonal matrix. The left orthogonal matrix U is POD modes and U is truncated to first L modes, where L is the number of dominant modes to keep. The truncated left orthogonal matrix $U_L \in \mathbb{R}^{N \times L}$is the optimal POD modes ϕ_L. The projections coefficients are found by performing scalar product between ϕ_L and S, which is used as output data to train the RBF regression model.

The inputs for the RBF regression model consist of primary inputs and IC of state variables $\left(\boldsymbol{P}_{\boldsymbol{p,init}}^{\boldsymbol{1\times 1}}, \boldsymbol{h}_{\boldsymbol{p,init}}^{\boldsymbol{1\times n}}, \boldsymbol{T}_{\boldsymbol{w,init}}^{\boldsymbol{1\times n}}, \boldsymbol{T}_{\boldsymbol{s,init}}^{\boldsymbol{1\times n}}\right)$. The IC for state variables, when stacked together, result in a vector of dimension 3n+1, with n being the number of control volumes. The lengthy IC will affect the performance of the RBF model. Thus, feature selection is applied using PCA, resulting in a reduced set of features denoted as IC_{red}. In this study, the RBF model's performance is studied for different number of principle components. The first 7 principal components are found to be adequate to effectively represent the spatial initial conditions of all state variables together. The RBF regression model is fitted between inputs $\xi = [h_{p,in}, \dot{m}_{p,in}, T_{s,in}, \dot{m}_{s,in}, IC_{red}]$ and the corresponding projection coefficients using least square method, and the optimal weights are found. The RBF regression model predicts new projection coefficients g_l given new input ξ_{new}.

3.2 Error Correction by Deep Neural Network

The ROM is built based on the data generated for the input steps of constant time length $t_{is,const}$. Thus, given an input, ROM predicts the solution for the receptive time length $t_{is,const}$. In order to have flexibility in the input step's time length as needed and to correct the error made by ROM in the quantity of interest, error correction unit is added which uses a DNN. It takes the quantity of interest from the ROM prediction along with the input of ROM and outputs the corrected quantity of interest. In the

https://doi.org/10.52202/077185-0088

context of dynamic modeling of heat exchanger, the quantity of interest is secondary fluid's (water) outlet temperature over time.

3.2.1 Data preparation for training DNN: New training data set D_2 is generated following the same procedure used to create the training data set D_1 for the ROM. A number of sequences of simulations are performed and each sequence has multiple continuous input step variations, but the key difference here lies in the time length of each input step. Unlike during data generation for ROM where time length of each input step is fixed to a constant $t_{is,const}$. Here the time length of the input step is not constant and it is chosen randomly within a range for each input step within a sequence. The varying time length of the input step is denoted as $t_{is,var}$. Selecting optimal bounds for the range of $t_{is,var}$ is crucial. The upper bound can be the time before the system begins to reach a steady state for each input combination. The lower bound is the minimum time length of the input step needed in prediction and model deployment stage. Thus, the upper and lower bounds of $t_{is,var}$ can be chosen based on the respective application and requirements. In this study, it was observed that the lower bound is, the more data is required during training to have good accuracy.

The data for training the DNN is collected as follows. Firstly, for the inputs corresponding to the training data set D_1 fed to ROM and high dimension solutions are predicted, and the water outlet temperature solution is extracted for respective inputs to train DNN. Even though ROM is built using training data set D_1, this is done so that the DNN learns to correct the error made by ROM specifically on its training data set D_1. Secondly, predicting the outputs for data set D_2, which is not straight forward as the ROM is built to predict solution for constant time length of an input step and in contrast, in D_2, the input step's time length is varying.

The validation of ROM for the input sequence with varying time lengths of input step is as follows. For each inputs step with time length being $t_{is,var}$, the corresponding inputs are given to the ROM and the solution is the prediction. The predicted solution is for time length of $t_{is,const}$. However, the required solution for a different time length $t_{is,var}$. If $t_{is,var} < t_{is,const}$, the solution of the state variables corresponding to time $t_{is,const}$ is trimmed till $t_{is,var}$. If $t_{is,var} > t_{is,const}$, the final solution of the state variables from the solution corresponding to $t_{i,const}$ is taken as IC, and once again given to ROM along with the same inputs, and solution is predicted. Now, in total, the predicted solution is for time length of $t_{is,const} + t_{is,const}$ and this predicted solution is trimmed till $t_{is,var}$. The final solution of current input step combination is given as IC for next input step and same process is repeated.

3.2.2 Training of DNN: The training set D_2 is collected by performing 20 sequences of simulations with each has 20 continuous input steps. The time length of each set of input step is varied randomly between 75 to 125 secs. The water outlet temperature data which is extracted from the predicted outputs for the inputs corresponding to training data D_1 and D_2 is combined with the ROM inputs and acts as training inputs for DNN. The corresponding training outputs will be the actual water outlet temperature data. The input format for DNN is $Input_{DNN} = \left[T_{s,out}\ , t\ , h_{p,in}\ , \dot{m}_{p,in}\ , T_{s,in}\ , \dot{m}_{s,in}\ , IC_{red}\right]_t$. The DNN learns to corrects the error made by ROM in the outlet water temperature $T_{s,out}$ time step by time step. The hyperparameters and other specifications of the DNN used is specified in Table 2. Overall, the ROM and error correction unit works together to predict corrected $T_{s,out}^{new}$.

Table 2: Hyperparameters for the DNN

No. of layers	5
No. of neurons per layers	100
Optimization	Adam
Activation function	Rectified Linear Unit (ReLU)

https://doi.org/10.52202/077185-0088

4 VALIDATION OF SURROGATE MODEL

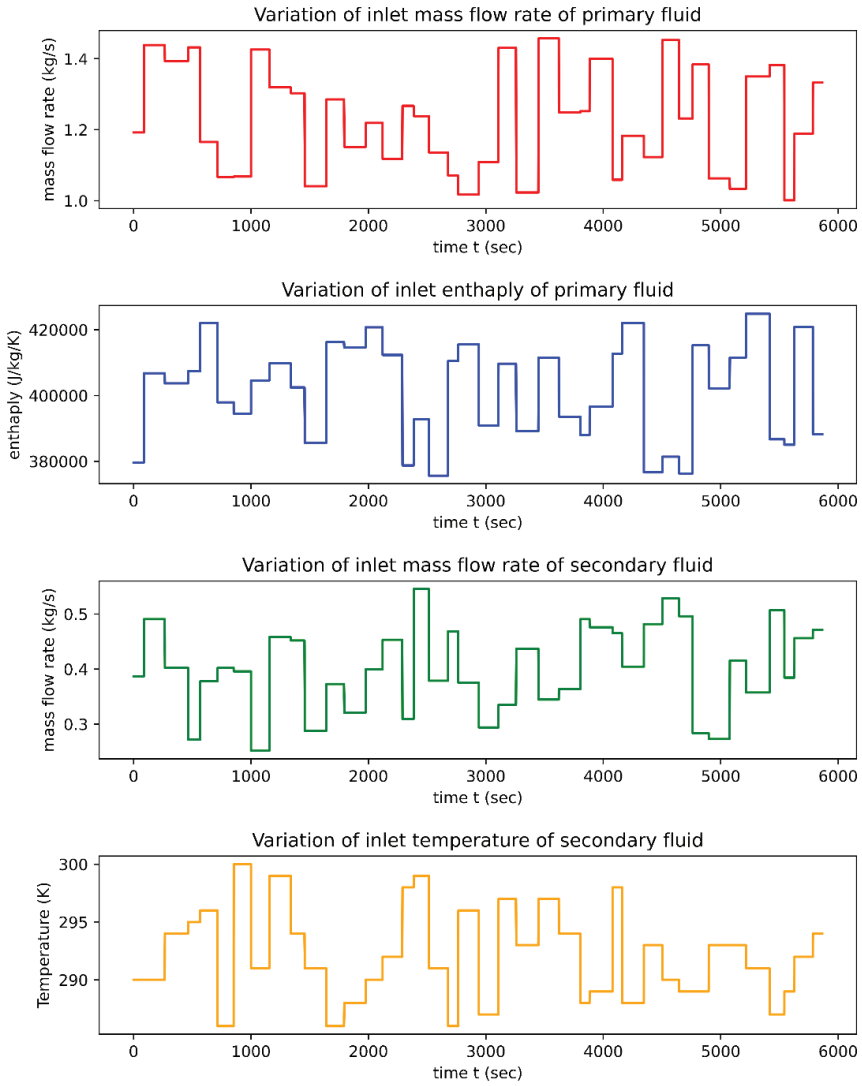

Figure 5: Variation of primary input parameters over time for validation sequence 1

The surrogate model is validated for two different validation sequences. In both sequences, the primary parameters such as $\dot{m}_{p,in}, \dot{m}_{s,in}, h_{p,in}, T_{s,in}$ are varied randomly in a step like manner within the given range as mentioned in Table 1. The time length of each input step is also randomly selected within the range 75 to 200 secs. Only the input variation for validation sequence 1 is shown in Figure 5.

Table 3: Comparative Error Metrics for Water Outlet Temperature between FV and Surrogate Model's solution across Validation Sequences

Validation Sequence	Mean Squared Error (K^2)	Maximum Absolute Error (K)	Mean Absolute Error (K)
1	0.16	1.97	0.31
2	0.25	2.26	0.38

https://doi.org/10.52202/077185-0088

From Table 3 and Figure 6, it is evident that the surrogate model exhibits quite good accuracy against FV on the water's outlet temperature. Even though there are some fluctuations in the surrogate model's solution, it captures the overall dynamics very well. The fluctuations and spikes primarily occur because the solution for a sequence of input steps is approximated iteratively, using the final solution of the previous step as the initial condition (IC) for the current step. Sometimes, the IC derived from the previous step's approximated solution may not be sufficiently accurate. However, in longer aspect, this does not significantly impact the overall accuracy of the surrogate model. From Table 4, in terms of computation time, the surrogate model outperforms the FV model with very large gap. The surrogate model is nearly 150 times faster than FV model. Overall, the surrogate model, featuring a simple and straightforward building and training process, predicts the quantity of interest at a significantly faster speed with good accuracy which is around 0.35(K) mean absolute error.

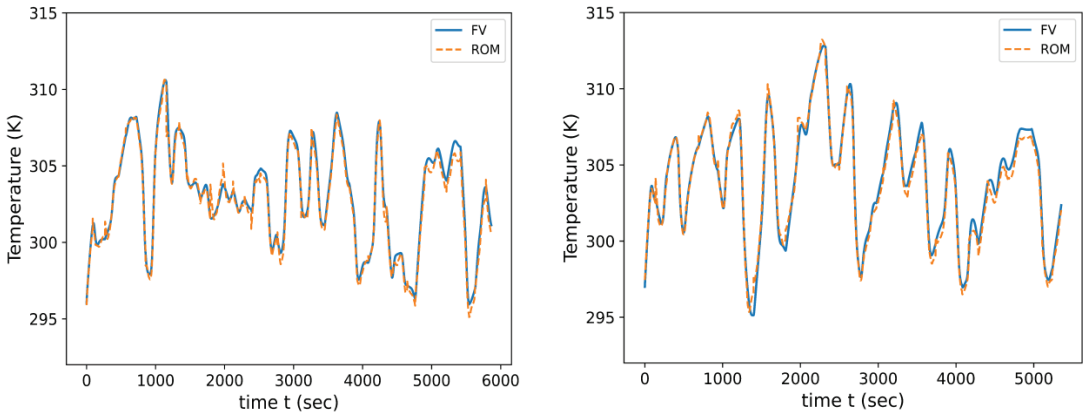

(a) (b)

Figure 6: Comparison of water outlet temperature solution over time between FV model and surrogate model for validation sequence 1 (a) and 2 (b)

Table 4: Computation time taken by FV model and surrogate model for different validation sequences

Validation Sequence	FV model	Surrogate model
1	986 sec	6.75 sec
2	1040 sec	6.72 sec

5 CONCLUSIONS

The surrogate model for dynamic heat exchanger, which employs non-intrusive ROM and an error correction unit, demonstrates superior performance and significant computational time savings, nearly 150 times compared to FV heat exchanger model. Furthermore, the surrogate model predicts the quantity of interest (water's outlet temperature) with a mean absolute error of around 0.35K, showcasing its compatibility for certain model control applications and system optimization. The potential future research aspects on this surrogate model are improving the model to have more flexibility in nature of input variation, improving the accuracy and making the model more generalized and robust by incorporating physics in the error correction unit.

NOMENCLATURE

v	velocity $(m\ s^{-1})$
t	time coordinate (s)
z	Spatial coordinate (m)

https://doi.org/10.52202/077185-0088

h	Enthalpy ($J\ kg^{-1}\ K^{-1}$)
P	Pressure (Pa)
A	Surface area (m^2)
T	Temperature (K)
C_p	Specific heat capacity ($J\ kg^{-1}\ K^{-1}$)
$\dot{m}$	Mass flow rate ($kg\ s^{-1}$)
V	Volume (m^3)
IC	Initial Conditions (-)
ρ	Density ($kg\ m^{-3}$)
α	Heat transfer Coefficient ($W\ m^{-2}K^{-1}$)
ϕ	Orthogonal modes (-)

Subscript

p	Primary fluid
s	Secondary fluid
w	Tube wall
in	Inlet
out	Outlet
is	Input step
init	Initial

ACKNOWLEDGEMENT

This work was carried out under the auspices of the ValaDoE chair at IMT Atlantique in partnership with Télécom Paris and Mines Saint Etienne, and was supported by Enedis, Région Pays de la Loire, Nantes Métropole and Akajoule.

REFERENCES

Alonso, D., Velazquez, A. and Vega, J., 2009, Robust reduced order modeling of heat transfer in a back step flow, *Int. J. Heat Mass Transf.*, vol. 52, no. 5-6: pp. 1149–1157.

Audouze, C., De Vuyst, F. and Nair, P.B., 2013, Nonintrusive reduced-order modeling of parametrized time-dependent partial differential equations, *Numer. Methods Partial Differ. Equ.*, vol. 29, no. 5: pp. 1587–1628.

Baldea, M. and Daoutidis, P., 2006, Model reduction and control of reactor–heat exchanger networks, *J. Process Control*, vol. 16, no. 3: pp. 265–274.

Bendapudi, S., Braun, J. E., & Groll, E. A., 2008, A comparison of moving-boundary and finite-volume formulations for transients in centrifugal chillers, *Int. J. Refrig.*, vol. 31, no. 8: pp. 1437-1452. doi:16/j.ijrefrig.2008.03.006.

Bell, I. H., Wronski, J., Quoilin, S., and Lemort, V., 2014, Pure and Pseudo-pure Fluid Thermophysical Property Evaluation and the Open-Source Thermophysical Property Library CoolProp, *Ind. Eng. Chem. Res.*

Bergmann, M., Cordier, L. and Brancher, J.P., 2005, Optimal rotary control of the cylinder wake using proper orthogonal decomposition reduced-order model, *Phys. Fluids*, vol. 17, no. 9: p. 097101.

Braun, J. E., 1988, Methodologies for the design and control of central cooling plants, University of Wisconsin, Madison, Ph.D. dissertation.

https://doi.org/10.52202/077185-0088

Chatterjee, A., 2000, An introduction to the proper orthogonal decomposition, *Curr. Sci.*, vol. 78, no. 7: pp. 808–817.

Chinesta, F., Ammar, A. and Cueto, E., 2010, Recent advances and new challenges in the use of the proper generalized decomposition for solving multidimensional models, *Arch. Comput. Methods Eng.*, vol. 17, no. 4: pp. 327–350.

Grald, E.W. and MacArthur, J.W., 1992, A moving boundary formulation for modeling time-dependent two-phase flows, *Int. J. Heat Fluid Flow*, vol. 13, no. 3: pp. 266-272.

Hardy, R.L., 1971, Multiquadric equations of topography and other irregular surfaces, *J. Geophys. Res.*, vol. 76, no. 8: pp. 1905–1915.

He, X.D., Liu, S. and Asada, H., 1994, A moving interface model of two-phase flow heat exchanger dynamics for control of vapor compression cycle heat pump and refrigeration systems design, analysis and applications, *AES Vol. 32*, ASME.

Jin, H., and Spitler, J. D., 2002, A parameter estimation based model of water-to-water heat pumps for use in energy calculation programs, *ASHRAE Transactions*, vol. 108, no. 1: pp. 3-17.

Johnson, R.M., 1963, On a theorem stated by Eckart and Young, *Psychometrika*, vol. 28, no. 3: pp. 259–263.

MacArthur, J.W. and Grald, E.W., 1987, Prediction of cyclic heat pump performance with a fully distributed model and a comparison with experimental data, *ASHRAE Transactions*, vol. 93, part 2: pp. 314-325.

Majumdar, R., Singh, S. and Saha, S.K., 2018, Quasi-steady state moving boundary reduced order model of two-phase flow for ORC refrigerant in solar-thermal heat exchanger, *Renew. Energy*, vol. 126: pp. 830–843.

Pettit, N.B.O.L., Willatzen, M. and Ploug-Sorensen L., 1998, A general dynamic simulation model for evaporators and condensers in refrigeration. Part II: simulation and control of an evaporator, *Int. J. Refrig.*, vol. 21, no. 5: pp. 404-414.

Rossi, T.M and Braun, J.E., 1999, A real-time transient model for air conditioners, *Proc. 20th Int. Congr. Refrig.*, IIF/IIR: pp. 743.

Samadiani, E. and Joshi, Y., 2010, Reduced order thermal modeling of data centers via proper orthogonal decomposition: A review, *Int. J. Numer. Methods Heat Fluid Flow*, vol. 20, no. 5: pp. 529–550.

Schmid, P. J., 2010, Dynamic mode decomposition of numerical and experimental data, *J. Fluid Mech.*, vol. 656: pp. 5–28.

Volkwein, S., 2013, Proper orthogonal decomposition: Theory and reduced-order modelling, *Lecture Notes, Univ. Konstanz*, vol. 4, no. 4: pp. 1–29.

Xu B., Yebi A., Hoffman, M., and Onori, S., 2018, A rigorous model order reduction framework for waste heat recovery systems based on proper orthogonal decomposition and Galerkin projection, *IEEE Trans. Control Syst. Technol.*, vol. 28, no. 2: pp. 635–643.

Zou, H., Hastie, T. and Tibshirani, R., 2006, Sparse principal component analysis, *J. Comput. Graph. Stat.*, vol. 15, no. 2: pp. 265–286.

https://doi.org/10.52202/077185-0088